

12th CIRP Conference on Photonic Technologies [LANE 2022], 4-8 September 2022, Fürth, Germany

Improvement of Charpy impact toughness by using an AC magnet backing system for laser hybrid welding of thick S690QL steels

Ömer Üstündag^{a,*}, Nasim Bakir^a, Andrey Gumenyuk^{a,b}, Michael Rethmeier^{c,a,b}

^aBundesanstalt für Materialforschung und -prüfung (BAM), Unter den Eichen 87, 12205 Berlin, Germany

^bFraunhofer Institute for Production Systems and Design Technology, Pascalstraße 8-9, 10587 Berlin, Germany

^cInstitute of Machine Tools and Factory Management, Technische Universität Berlin, Pascalstraße 8-9, 10587 Berlin, Germany

* Corresponding author. Tel.: +49-30-8104-3150; E-mail address: oemer.uestuendag@bam.de

Abstract

The study deals with the influence of the heat input and the resulting cooling times on the microstructure and Charpy impact toughness of single-pass laser hybrid welded 20-mm thick high-strength steel S690QL. The main focus is on the change of the mechanical properties over the entire seam thickness. The cooling times were measured in-situ using a pyrometer and an optical fibre in three different depths of the seam where Charpy impact test specimens were also later taken. Thereby, three different heat inputs from 1.3 kJ/mm to 2 kJ/mm were investigated. Despite the observed decreased values of both $t_{8/5}$ -cooling time and the Charpy impact toughness in the root part of the seam, the required impact toughness of 38 J/cm² could be reached in dependence on applied heat input, especially at the heat input of 1.6 kJ/mm.

© 2022 The Authors. Published by Elsevier B.V.

This is an open access article under the CC BY-NC-ND license (<https://creativecommons.org/licenses/by-nc-nd/4.0>)

Peer-review under responsibility of the international review committee of the 12th CIRP Conference on Photonic Technologies [LANE 2022]

Keywords: laser hybrid welding; AC magnet backing; Charpy impact toughness; high-strength steel; S690QL

1. Introduction

The laser hybrid welding process is the coupling of the laser beam welding (LBW) process and the arc welding process, mostly gas metal arc welding process (GMAW) in a common interaction zone and was developed in the end of the 1970s [1]. The advantages of the laser hybrid welding are the high penetration depth due to the high power density of the laser beam and thus resulting reduction of the welding time and layer number when welding thick-walled components, better gap bridgeability compared to pure LBW process, reduction of the heat input compared to GMAW process and resulting lower distortion. One of the disadvantages of the process is the high cooling rate compared to the GMAW process, which can lead to decreased mechanical properties such as Charpy impact toughness, hardening in the fusion zone or heat affected zone especially when welding high strength steels (HSS). The HSS

are characterized by their fine grained structure and a combination of micro-alloying together with quenching and tempering, which gives the steel its properties such as high strength and toughness. The structure mainly consists of martensite and bainite [2]. The joining of HSS presents some challenges regarding the thermal cycle of the welding process, as the material properties can be changed under heat influence.

The high welding speeds at LBW lead to high solidification and cooling rates, which may in turn lead to pores or cracking in the weld. The rapid cooling rate could also result in the increase of hardness in the weld and heat-affected zone [3] as well as changes of the microstructure and mechanical properties through the fusion zone and the HAZ. On the other hand, a high heat input such as at the arc welding processes can lead to grain-coarsening, so that the mechanical properties can be deteriorated. The heat input is the major parameter affecting the cooling rate and thus the microstructure and the mechanical

properties. So, it has to be controlled by suitable selecting welding parameters and particularly a welding speed.

In numerous studies, the HLAW is a proper welding process for welding of HSS due to its low heat input and the possibility to influence the microstructure via suitable selecting of the filler wire. It is reported that with a heat input of 0.43 kJ mm^{-1} to 0.51 kJ mm^{-1} at HLAW of 10 mm thick S690QL steels, the minimum required Charpy impact toughness could be reached and the hardness of the weld metal and HAZ had a small variation from the base metal without any preheating [4]. In [5] the influence of filler wire on the mechanical properties was investigated for single-pass welded 6 mm thick ultra-high strength steels. Alloyed (matching) and non-alloyed undermatching filler wire were applicable to weld with adequate impact toughness at $-40 \text{ }^\circ\text{C}$ temperature for heat inputs between 0.31 kJ mm^{-1} and 0.63 kJ mm^{-1} . Grünenwald et al. [6] reported that solid wire is appropriate for welding of up to 14.5 mm thick high-strength steels regarding the Charpy impact toughness. On the other hand, Rethmeier et al. [7] reached the conclusion that high quality welds with appropriate ductile-to-brittle-transition can be produced by metal cored wire when the heat input was about 0.9 kJ mm^{-1} to 1 kJ mm^{-1} . However, the studies were performed on pipeline steels, the strength level is comparable to S690QL steels.

As the state of the art also shows, the single-pass HLAW of HSS poses some challenges. The aim of this study is to determine the influence of the heat input on the mechanical properties of single-pass HLAW 20 mm thick S690QL steels. Thereby, the mechanical properties will be studied in different depths of the single-pass welds because they can vary over the thickness as reported in [8] due to the inhomogeneous local thermal cycles, uneven cooling conditions over the depth and the irregular distribution of the elements of filler wire. To avoid root defects such as sagging or the formation of drop-outs, a contactless electromagnetic backing is used. The effectiveness of the contactless electromagnetic backing was demonstrated by several studies [9-11] for single-pass HLAW of steels with a wall thickness up to 30 mm.

2. Experimental setup

For this study, the high-strength steel S690QL with a material thickness of 20 mm was used. All welds were butt-joint welded in a single-pass. A low-alloyed solid wire Union X85 (G 79 5 M21 Mn4Ni1,5CrMo according to EN ISO 16834-A) with a diameter of 1.2 mm was used as filler wire. A mixture of argon with 18% CO_2 with a flow rate of 20 l min^{-1} served as shielding gas. The materials used, and their chemical compositions are shown in Table 1.

Table 1. Chemical composition of materials used, shown in wt%.

Material / Element	C	Si	Mn	Cr	Mo	Ni	P
S690QL	0.2	0.8	1.7	1.5	0.7	2	0.02
Union X85	0.09	0.7	1.7	0.3	0.6	1.85	-
	S	V	Al	Cu	Nb	Ti	Fe
S690QL	0.01	0.12	0.015	0.5	0.06	0.05	bal.
Union X85	-	-	-	-	-	-	bal.

The mechanical properties of the materials used are shown in Table 2.

Table 2. Mechanical properties of materials used.

Material	Yield Strength in MPa	Tensile Strength in MPa	Elongation A5 in %	Impact energy in J
S690QL	690	770-930	14	30 (-40°C)
Union X85	790	880	16	47 (-50°C)

The welding tests were performed with a 20 kW Yb fiber laser YLR 20000, with a wavelength of $1.06 \text{ } \mu\text{m}$ - $1.07 \text{ } \mu\text{m}$ and a beam parameter product of 11.2 mm x mrad in flat position (1G). The laser radiation was transmitted through an optical fiber with a core diameter of $200 \text{ } \mu\text{m}$. A laser processing head BIMO HP from HIGHYAG with a focal length of 350 mm providing a spot focus diameter of 0.56 mm was used. The Qineo Pulse 600A welding unit served as the current source for arc welding and was operated in pulse mode with a frequency of 180 Hz. The GMA torch was tilted 25° relative to the laser axis, where the laser axis was positioned 90° to the surface of weld specimens. All tests were carried out with an arc leading orientation. The distance between the wire tip extension and the spot of the laser beam on the workpiece was defined as 4 mm. The focal position of the laser beam relative to the workpiece surface was of -5 mm . The welding speed was changed from 0.75 m min^{-1} to 1.7 m min^{-1} so that the heat input was varied between 1.3 kJ mm^{-1} and 2 kJ mm^{-1} . The variable welding parameters are listed in Table 3.

Table 3. Mechanical properties of materials used.

	Laser beam power in kW	Welding speed in m min^{-1}	Wire feed speed in m min^{-1}	Heat input in kJ mm^{-1}
Case 1	20.1	1.7	15	1.3
Case 2	17.7	1.2	13	1.6
Case 3	16.1	0.75	9	2

During the experiments a contactless electromagnetic backing was used. The AC magnet was 2 mm under the workpiece in a fixed position. The movement of the workpiece for welding was realized via external axis. The distance between the two magnetic poles was 25 mm. Depending on the material thickness and high hydrostatic pressure, the AC magnet was operated with an oscillating frequency of 1.21 kHz and a power of $1.7 \text{ kW} \pm 200 \text{ W}$.

The temperature measurements during welding were performed with help of two two-color pyrometers, which were focused on two collimators with a numerical aperture (NA) of 0.25 and spectral range of 1050 nm to 1600 nm. Two optical fibres with a core diameter of $550 \text{ } \mu\text{m}$, NA of 0.22 operating in the wavelengths range of 400 nm to 2200 nm were fixed each to the collimator. The second free edge of the optical fibers were put in the material, which were prefabricated with holes, to measure the cooling time during welding inside the material and the root part. Fig. 1 demonstrates the experimental setup of a HLAW welding process with a contactless electromagnetic backing.

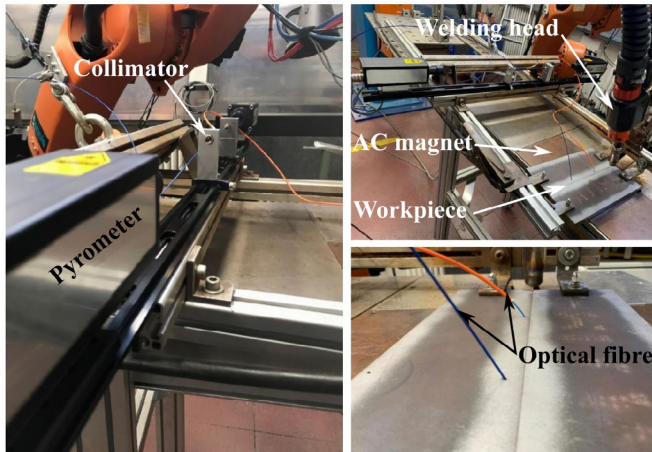


Fig. 1. Experimental setup

Subsequently, for the investigation of the mechanical properties, hardness maps were carried out. Additionally, sub-sized (5 mm x 10 mm x 55 mm) V-notched Charpy impact specimens in three different depths (arc-dominated zone, middle and laser-dominated zone) are extracted from the material with a notch in the fusion zone (FZ) and then tested at a testing temperature of $-20\text{ }^{\circ}\text{C}$. Also, flat tensile test specimens with a thickness of 5 mm were extracted from the arc-dominated zone and laser-dominated zone. The dimensions of the tensile test specimens correspond to the Form E according to DIN 50125.

3. Results

S690QL steel plates with a thickness of 20 mm could be welded in square groove butt joint configuration in a single-pass with three different heat inputs. With help of the contactless electromagnetic backing, sagging and gravity dropouts could be avoided even for lower welding speeds, so that all the welds could be classified in the highest evaluation group B according to EN ISO 12932 regarding the outer appearance of the seams. Exemplarily, one cross section for each case is shown in Fig. 2. It is evident that the seam geometry changes considerably at the different heat inputs. At higher welding speeds, the seam is very narrow, and the flanks are almost parallel, so that this weld can be more critical to cracks due to this geometry.

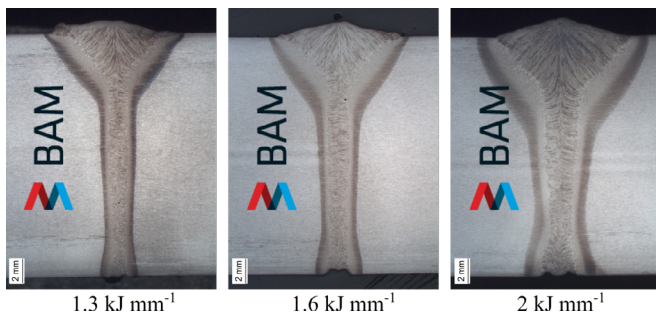


Fig. 2. Cross-sections of the single-pass laser hybrid welded 20 mm thick S690QL plates with different heat inputs and contactless electromagnetic backing

The cooling times from $800\text{ }^{\circ}\text{C}$ to $500\text{ }^{\circ}\text{C}$, the so-called $t_{8/5}$ -time, were measured on the top of the workpiece, in the middle with a horizontal distance of 2 mm to the edge and in the root with a distance of 2 mm each to the edge end to the bottom of the workpiece. The $t_{8/5}$ -time for the Case 1 with the lower heat input is decreased from 3.7 s on the top to 2.3 s and 1.9 s in the middle and the bottom, respectively. It can be recognized that the cooling time decreases over the thickness. The additional heat input from the arc welding process has a low impact to the root, which can be a limitational factor for single-pass HLA of thick plates in regard to the mechanical properties. The measured $t_{8/5}$ -times for all cases are summarized in Table 4. Exemplarily, the course of the $t_{8/5}$ -times for Case 2 in three different positions over the thickness are shown in Fig. 3.

Table 4. Measured $t_{8/5}$ -times for all cases in the three different depths.

	$t_{8/5}$ -time on the top surface in s	$t_{8/5}$ -time in the middle in s	$t_{8/5}$ -time in the root part in s
Case 1	3.7	2.3	1.9
Case 2	4.4	2.8	2
Case 3	8.2	6.4	4.1

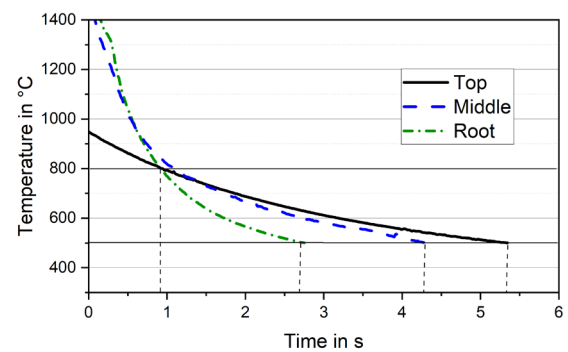


Fig. 3. Measured $t_{8/5}$ -times via pyrometer and optical fibre on the top, the middle and the root for Case 2.

The Vickers hardness were measured for the three cases using the UCI method. It is recognizable, that the hardness in the FZ reaches a maximum of up to 460 HV0.5 especially at high welding speeds of approx. 1.7 m min^{-1} . At the lower welding speeds, a hardening in the HAZ can be detected.

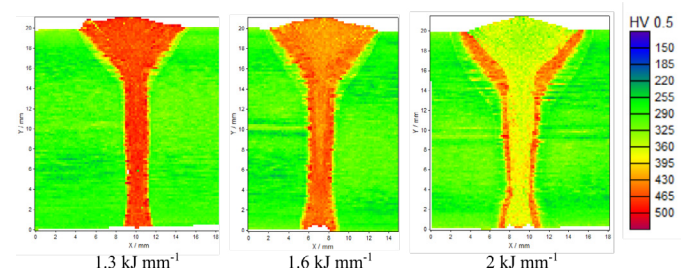


Fig. 4. Hardness maps of the single-pass laser hybrid welded 20 mm thick S690QL plates with different heat inputs and contactless electromagnetic backing

The results of the notched-bar impact test according to EN ISO 148-1 is shown in Table 5. The minimum required impact toughness (α_k) was 38 J cm^{-2} at a testing temperature of $-20\text{ }^{\circ}\text{C}$. The results of the Charpy impact tests are summarized in Table 5.

Table 5. Results of the Charpy impact tests; n = 5.

	Top KV in J (ak top in J cm ⁻²)	Middle KV in J (ak middle in J cm ⁻²)	Bottom KV in J (ak bottom in J cm ⁻²)
Case 1	45±5 (113±13)	27±17 (68±43)	45±25 (113±63)
Case 2	58±4 (145±10)	40±8 (99±20)	50±1 (125±3)
Case 3	17±2 (43±5)	23±8 (57±20)	17±1 (43±3)

It is recognizable that the Charpy impact toughness for Case 3 is lower than for the other samples. One reason for this is the effect of grain-coarsening due to the higher heat input. It can be further seen that the values of the Charpy impact toughness are comparable over the material thickness, contrary to the results in [8]. However, the observations in [8] were made for higher wall thicknesses. Additionally, the impact toughness in Case 1 shows higher standard deviations in the middle of the thickness and root part. One possible reason for that is, that cracks were observed on the tested specimens. Exemplarily, a tested specimen with a detected crack (Case 1, middle) and a tested specimen with a high impact toughness (Case 2, root) with a brittle-ductile mixed fracture are shown in Fig. 5.

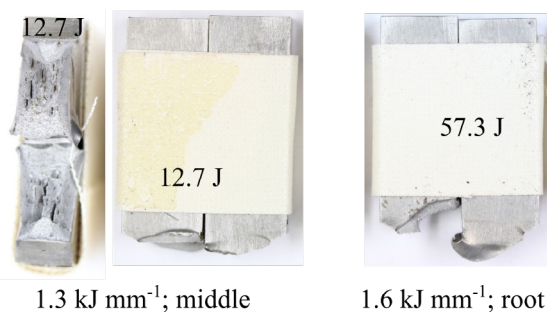


Fig. 5. Tested Charpy impact test specimens: brittle fracture (left) with cracks and brittle-ductile mixed fracture (right).

All tested tensile test specimens (arc-dominated zone as well as laser-dominated zone) reach the minimum required tensile strength of the base metal and are fractured at 828 MPa to 886 MPa. The fracture position is in the base metal, as it can be seen in the Fig. 6, exemplarily. The transverse tensile tests were each repeated three times for each of the three investigated heat inputs on for the two zones.



Fig. 6. Tested Charpy impact test specimens: brittle fracture (left) with cracks and brittle-ductile mixed fracture (right).

4. Summary

It could be shown that 20 mm thick high-strength steels of grade S690QL could be welded with the laser hybrid welding process in a single-pass by using a 20 kW fibre laser.

A contactless electromagnetic backing was used to prevent sagging. This had the advantage that the heat input could be varied by adaptation of the welding speed and the welding parameters to find an optimal range, where the mechanical properties such as Charpy impact toughness and tensile strength of the welds reaches the minimum required values. A heat input of 1.6 kJ mm⁻¹ can be recommended for single-pass welds of 20 mm thick S690QL steels. At higher welding speeds the crack formation could be observed, where at lower welding speeds the Charpy impact toughness was lower due to the phenomenon of grain-coarsening.

Acknowledgements

The research project was carried out in the framework of the Industrial Collective Research programme (IGF No.20.827N). It was supported by the Federal Ministry for Economic Affairs and Energy (BMWi) through the AiF (German Federation of Industrial Research Associations e.V.) based on a decision taken by the German Bundestag. Financial funding is gratefully acknowledged.

References

- [1] Eboo, M., Steen, W. M., Clarke, J. (1978). Arc Augmented Laser Welding. Conference Proceedings of the 4th Intern. Conference of Advances in Welding Processes, Volume 17, p. 257-265.
- [2] Hanus, F., Schröter, F., Schütz, W. (2005). State of art in the production and use of high-strength heavy plates for hydropower applications. Proceedings of the High Strength Steel for Hydropower Plants, Graz, Austria, 5-6.
- [3] Sokolov, M., Salminen, A., Kuznetsov, M., Tsubulskiy, I. (2011). Laser welding and weld hardness analysis of thick section S355 structural steel. Materials & Design, 32(10), 5127-5131.
- [4] Laitinen, R., Siltanen, J., Porter, D., Kömi, J. (2009). Laser-MAG Hybrid Welding of Direct Quenched High Strength Steel Grade S690QL. In Proceedings of the 12th Nordic Laser Materials Processing Conference (NOLAMP), August, Copenhagen, Denmark.
- [5] Siltanen, J., Kömi, J., Laitinen, R., Lehtinen, M., Tihinen, S., Jasnau, U., Sumpf, A. (2011). Laser-GMA hybrid welding of 960 MPa steels. In International Congress on Applications of Lasers & Electro-Optics (Vol. 2011, No. 1, pp. 592-598). Laser Institute of America.
- [6] Grünenwald, S., Seefeld, T., Vollertsen, F., Kocak, M. (2010). Solutions for joining pipe steels using laser-GMA-hybrid welding processes. Physics Procedia, 5, p. 77-87.
- [7] Rethmeier, M., Gumenyuk, A., Gook, S. (2008). Laser-hybrid welding for pipe production and pipe laying of thick large diameter. Proceedings of the 7th Asia-Pacific International IIW Congress, July, Singapore. p. 417-423.
- [8] Üstündağ, Ö., Gook, S., Gumenyuk, A., Rethmeier, M. (2019). Mechanical properties of single-pass hybrid laser arc welded 25 mm thick-walled structures made of fine-grained structural steel. Procedia Manufacturing, 36, 112-120.
- [9] Avilov, V. V., Gumenyuk, A., Lammers, M., Rethmeier, M. (2012). PA position full penetration high power laser beam welding of up to 30 mm thick AlMg3 plates using electromagnetic weld pool support. Science and technology of Welding and Joining, 17(2), 128-133.
- [10] Üstündağ, Ö., Fritzsche, A., Avilov, V., Gumenyuk, A., Rethmeier, M. (2018). Hybrid laser-arc welding of thick-walled ferromagnetic steels with electromagnetic weld pool support. Welding in the World, 62(4), 767-774.
- [11] Üstündağ, Ö., Avilov, V., Gumenyuk, A., Rethmeier, M. (2018). Full penetration hybrid laser arc welding of up to 28 mm thick S355 plates using electromagnetic weld pool support. In Journal of Physics: Conference Series (Vol. 1109, No. 1, p. 012015). IOP Publishing.